Materials Transactions, Vol. 45, No. 5 (2004) pp. 1687 to 1692

Influence of Purity on the Formation of Cube Texture in Aluminum Foils for Electrolytic Capacitors

Naoki Takata[1,*], Ken-ichi Ikeda[2], Fuyuki Yoshida[2], Hideharu Nakashima[2] and Hiroshi Abe[2]

[1]*Interdisciplinary Graduate School of Engineering and Science, Kyushu University, Fukuoka, 816-8580, Japan*
[2]*Faculty of Engineering Sciences, Kyushu University, Fukuoka, 816-8580, Japan*

In the present study, the crystal orientation and residual strains in hot rolled sheets, cold rolled foils, partially annealed foils, and additionally rolled foils of aluminum of 99.9% (3NAl) and 99.99% (4NAl) purity used for the fabrication of electrolytic capacitors, were evaluated by the SEM/EBSP method. The additionally rolled foils were annealed at 573 K and the behavior of the growth of cube-oriented grains and the grain boundary character were analyzed. In the hot rolled sheets and the partially annealed foils, cube-oriented grains in 4NAl were larger in number and size than those of 3NAl. From the result, it was clarified that purity of the aluminum affected the growth of cube-oriented grains during the thermo-mechanical treatment. In the additionally rolled foils annealed at 573 K, the growth of the cube-oriented grains in 4NAl was faster than that in 3NAl. In both 3NAl and 4NAl, the residual strains and the grain boundary character were similar. Accordingly, it is concluded that impurity in 3NAl could have segregated at the grain boundaries around cube-oriented grains and supressed the growth of cube-oriented grains.

(Received July 7, 2003; Accepted February 23, 2004)

Keywords: *high purity aluminum foil, recrystallization, cube texture, scanning electron microscope-electron back-scattering diffraction pattern (SEM-EBSP) method, impurity*

1. Introduction

In order to improve the capacitance of high voltage electrolytic capacitors, it is required to increase the surface area of high purity aluminum foils.[1,2] Cube texture ($\{100\}\langle001\rangle$)[3] is effective to increase the surface area through an etching process, because the etch pits form along crystallographic $\langle001\rangle$-direction into the foils. Accordingly, the aluminum foils for the electrolytic capacitors have a strong component of cube texture. To produce such foils, it is essential to apply particular thermo-mechanical treatment (partial annealing and additional rolling) between cold rolling and final annealing.[4]

The aluminum foils of 99.9% and 99.99% purity are used for practical electrolytic capacitors. But there is a problem that the density of cube-oriented grains is reduced when the lower purity aluminum foils are used.[5,6] It is suitable to use aluminum foils with lower purity from the viewpoint of the production cost. Therefore, it is important to clarify the reason why the density of cube-oriented grains change depending on the purity of aluminum. However, there are a lot of unresolved problems about the influence of purity on the cube texture of aluminum foils. The effect of production process and the mechanism of oriented growth of cube-oriented grains in the aluminum foils have been studied by several authors,[7–10] but there are few investigations of the effect of purity on the formation of cube texture after each process.

The purpose of this study is to investigate the influence of purity on the cube texture in aluminum foils for the electrolytic capacitors. For this purpose, aluminum foils of 99.9% and 99.99% purity for electrolytic capacitors were analyzed by SEM/EBSP method after each production process, compared with the results of 99.99% purity by Ikeda *et al.*[7] Based on these results, the influence of purity on the cube texture has been investigated placing emphases on the distribution of cube-oriented grains, residual strain and grain boundary character which contribute to the growth of cube-oriented grains.

2. Experimental Procedure

2.1 Samples

Aluminum foils of 99.9% and 99.99% purity as common samples of Branch Research Committee on Physical Metallurgy Related to Grain Boundaries, Japan Institute of Light Metals, were used as the samples for the present study. Hereafter, foils of 99.9% and 99.99% purity will be denoted as 3NAl and 4NAl, respectively. 3NAl contained 16 ppm Fe, 20 ppm Si and 40 ppm Cu, 4NAl contained 8 ppm Fe, 8 ppm Si and 50 ppm Cu.

In the present study, four kinds of samples, *i.e.*, hot rolled sheets, cold rolled foils, partially annealed foils and additionally rolled foils, were used. Hot rolled sheets, 7 mm in thickness, were cold rolled to 400 μm then to 130 μm in thickness. In the partial annealing process, 3NAl and 4NAl were annealed at 523 K and 503 K respectively, for 6 hours in air. The temperature was the most suitable condition for the formation of strong cube texture, which depends on the impurity in samples. The partially annealed foils were then cold rolled to 110 μm in thickness. The foils will be called as additionally rolled foils. These samples were taken at each preparation process. The preparation process of samples was shown in Fig. 1.

2.2 Observation by SEM/EBSP method

The local crystal orientation of samples was evaluated by SEM/EBSP (Electron Back-Scattering diffraction Pattern) method. The transverse section of hot rolled sheets was cut into 70 mm in the normal direction and 5 mm in the rolling direction. The normal plane of cold rolled foils, partially annealed foils (at 523 K in 3NAl and at 503 K in 4NAl respectively, for 6 hours) and additionally rolled foils (17% reduction in thickness) were cut into a sheet of $5 \times 10\,\text{mm}^2$.

*Graduate Student, Kyushu University

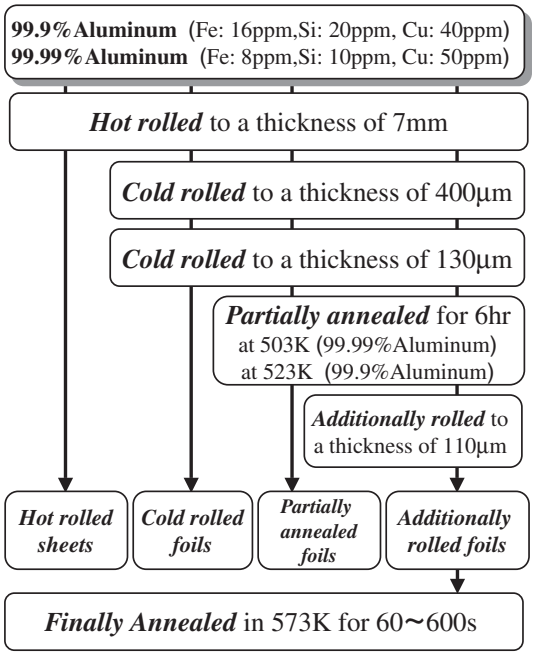

Fig. 1 Preparation process of samples.

With regard to the additionally rolled foils, the analysis was preformed focusing on the change of the texture during the final annealing. The final annealing was carried out in vacuum of 2×10^{-3} Pa and the temperature was risen at a rate of 1.5~1.7 K/s, then kept at 573 K for 60~600 seconds. The surface of samples was electropolished with a mixture of perchloric acid, ethylene glycol and ethyl alcohol of 1:2:7 in volume ratio. The polishing was carried out at 275 K with the DC voltage of 23 V.

EBSP analysis was carried out using SEM (JEOL JSM-5310, W-filament), equipped with TSL OIM (Orientation Imaging Microscopy) system at 25 kV. The scanning step was 1~5 μm. In order to analyze the texture of the hot rolled sheet from the surface to the center in depth direction, the area of 1000 μm × 100 μm of TD plane was measured. For other samples, ND planes were analyzed with the scanning area of 100~200 μm in the rolling direction and 400~1000 μm in the transverse direction.

In order to analyze the grain boundary characters, the common axis and the rotation angle between the adjacent grains were calculated by a program developed by the authors. From the results, Σ value was determined based on the coincidence site lattice theory.[11,12] In the present study, $\Sigma 3 \sim \Sigma 27$ boundaries were defined as the coincidence boundaries. The common axis obtained by the calculation, which was applied to the nearest index of 13 indices using an integral number from 0 to 3, as $\langle 001 \rangle$, $\langle 011 \rangle$, $\langle 012 \rangle \cdots \langle 223 \rangle$ and $\langle 233 \rangle$. The allowed deviation angle between the calculated axis and the applied axis was 8 degrees, not depend on the Σ value of coincidence boundaries. And as the rotation angle, the Brandon criterion[7,11] was applied for the tolerance of the coincidence boundaries, that is represented the following equation.

$$\Delta\omega = \frac{15}{\sqrt{\Sigma}} \quad (1)$$

where, Σ denotes Σ value of coincidence boundaries, $\Delta\omega$ (degree) is the maximum allowance of deviation from the exact coincidence orientation. The boundaries whose rotation angle was smaller than 15 degrees were defined as the low-angle boundary. The high-angle boundaries except for the low Σ coincidence boundaries were defined as the random boundaries. In the present study, attention was focused on the growth of cube-oriented grains. The cube-oriented grains were defined as the grains whose misorientation from ideal cube-orientation ($\{100\}\langle 001 \rangle$) is less than 15 degrees. Therefore, the grain boundaries of cube-oriented grains were classified into the coincidence boundaries and the random boundaries. Based on these definitions, the maps of grain boundary character distribution were prepared.

2.3 Vickers hardness test

The Vickers hardness of all samples was measured using Akashi MVK-H1 Hardness Tester for the evaluation of the residual strain. The indentation was carried out five times for each sample at 294 K with the load of 9.8×10^{-2} N for 15 seconds.

3. Results and Discussion

3.1 Distribution of cube-oriented grains in hot rolled sheets and cold rolled foils

Figure 2 shows the analyzed areas in hot rolled sheets. Figures 3 and 4 show the OIM images for crystal orientation, indicating cube-oriented grains in the hot rolled sheets of 3NAl and 4NAl, respectively. (a) and (b) in Fig. 3 and Fig. 4 are the surface areas. (c) and (d) in Figs. 3 and 4 are the areas which are about 3 mm in depth under the surface. In these figures, the longitudinal direction is ND and the horizontal direction is RD. The OIM images for crystal orientation shown Figs. 3(a) and (c) and Figs. 4(a) and (c) are colored according to the unit triangle, which corresponds to the inverse pole figure of ND. These results show that the bands consisted of the same oriented grains in the hot rolled sheets were stratified along the ND and the width of bands was 50~200 μm. On 3NAl, the major components of crystal orientations to ND were {111} and {112} in the surface layer and {101} in the center layer. On the other hand, the major components of crystal orientation to the ND on 4NAl were {112} and {001} in the surface layer, and was {111} and {101} in the center layer. In particular, Brass orientation ($\{110\}\langle 112 \rangle$), Copper orientation ($\{112\}\langle 111 \rangle$) and S-orientation ($\{123\}\langle 634 \rangle$) which usually formed in aluminum as rolled texture (β-fiber),[13] were observed not in the surface area but in the interior. It was considered that the deformation behavior during the hot rolling would change along the

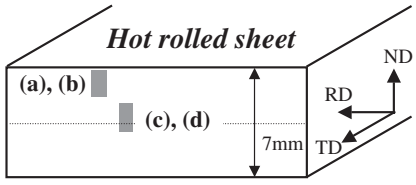

Fig. 2 Schematic illustration for analyzed area on hot rolled sheets, shown in Fig. 3 and Fig. 4.

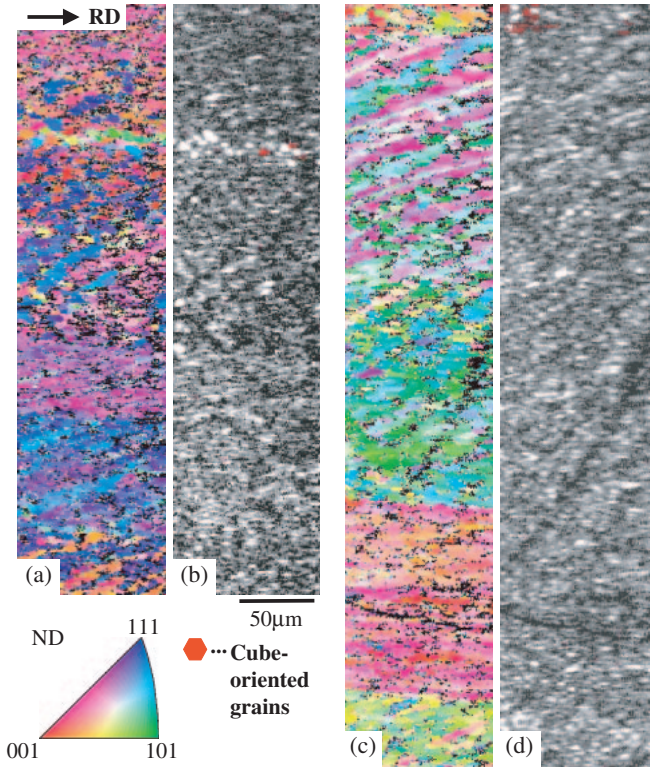

Fig. 3 The OIM images for (a) crystal orientations and (b) cube-oriented grains in the surface layer, and the OIM images of (c) crystal orientations and (d) cube-oriented grains in the centered layer of the hot rolled sheets of 3NAl.

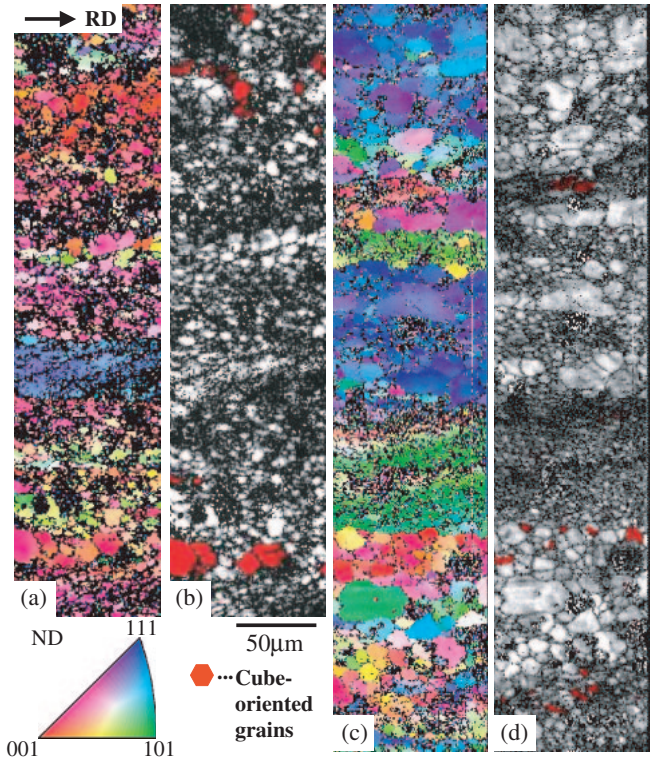

Fig. 4 The OIM images for (a) crystal orientations and (b) cube-oriented grains in the surface layer, and the OIM images of (c) crystal orientations and (d) cube-oriented grains in the centered layer of the hot rolled sheets of 4NAl.

ND,[14] which cause the differences in textures. It was also observed that 3NAl consist of finer and more homogeneously distributed grains than those in 4NAl. And some coarsened grains whose size was 20~40 μm were locally observed in 4NAl. While in 3NAl, such coarsened grains were not observed and the average grain size was about 5 μm. From these results, it was considered that 4NAl could have recovered or recrystallized during hot rolling more easily than 3NAl, because 3NAl contains more Fe and Si than 4NAl. The impurities are known to reduce the mobility of grain boundaries and suppressed the grain boundary migration in dynamic recrystallization.[15]

The OIM images for cube-oriented grains are shown in Figs. 3(b) and (d) and Figs. 4(b) and (d). In these images, red grains represent cube-oriented grains. The average size of cube-oriented grains was 8.5 μm in 4NAl and 3.3 μm in 3NAl, respectively. The number of cube-oriented grains in 4NAl is larger than that in 3NAl. As seen in the images, there were cube-oriented grains along the rolling direction in the surface layer and in the center layer both in 3NAl and 4NAl. Endo and Inagaki[16] also reported that the cube-oriented grains were detected in the center layer of 4NAl using the X-ray diffraction methods. In this study, it was revealed that cube-oriented grains existed in not only the center layer but

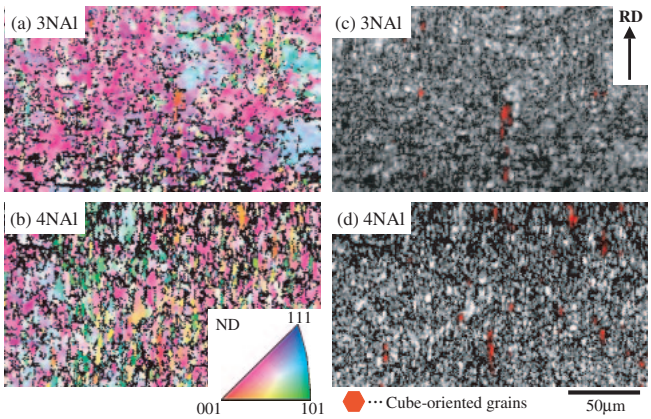

Fig. 5 The OIM images for (a)(b) crystal orientations and (c)(d) cube-oriented grains in the surface of cold rolled foils of 3NAl and 4NAl.[7]

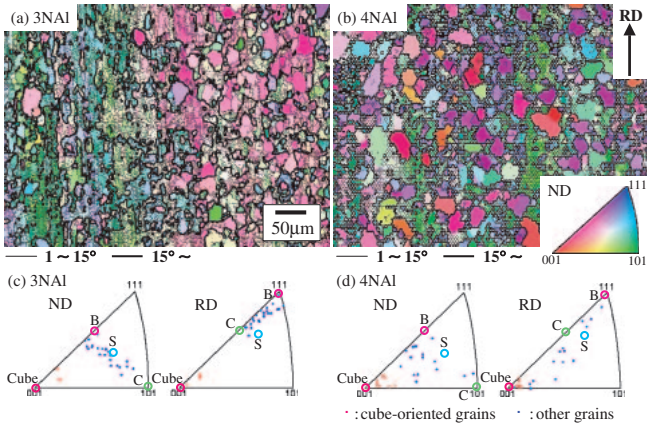

Fig. 6 The OIM images for crystal orientations differences in the surface of partially annealed foils of (a) 3NAl and (b) 4NAl, and inverse pole figure for the strain-free grains in partially annealed foils of (c) 3NAl and (d) 4NAl.

also the surface layer of hot rolled sheets.

Figure 5 shows the OIM images for the crystal orientation and the cube-oriented grains in the region close to the surface of cold rolled foils of 3NAl and 4NAl.[7] The longitudinal and horizontal directions are represented by RD and TD, respectively. Figures 5(a) and (b) show that there are a number of green, purple and sky blue colored grains, which correspond to Brass orientation, Copper orientation and S-orientation respectively, both in 3NAl and 4NAl. The main component of orientation in the cold rolled foils was Copper orientation on both 3NAl and 4NAl, but the some areas with Brass orientation were observed in 4NAl. The results shows that β-fiber as a typical cold rolled texture was formed by a heavy cold rolling with the reduction as much as 97%. The cube-oriented grains, about 3 μm in diameter, were observed both in 3NAl and 4NAl. The number of cube-oriented grains was larger in 4NAl than in 3NAl, reflecting the fact that the number of cube-oriented grains in 4NAl was larger than that in 3NAl after hot rolling, as shown in Figs. 3 and 4. Consequently, it could be concluded that the distribution of cube-oriented grains in cold rolled foils attributes to that in hot rolled sheets.

3.2 Distribution of recovered and recrystallized grains in the partially annealed foils

Figures 6(a) and (b) show the OIM images for the crystal orientation and the local orientation difference in partially annealed foils of 3NAl and 4NAl. Each crystal orientation is represented by the unique color according to the unit triangle. Fine lines indicate that the misorientation angle between adjacent scanning points is 1∼15 degrees, while bold lines indicate that the angle is over 15 degrees. Compared with the cold rolled foils, the grain is coarsened after partial annealing. The grain size of 4NAl was larger than that of 3NAl in the partially annealed foils. This result shows that the behavior of grain growth during partial annealing differed due to the purity of foils. 4NAl had more cube-oriented grain than 3NAl. It is considered that the distribution of cube-oriented grains in the partially annealed foils is influenced by not only impurity but also the distribution of cube-oriented grains in cold rolled foils. With respect to the β-fiber component, Copper orientation occupied more 40% on the surface of both 3NAl and 4NAl.

In Figs. 6(a) and (b), bold lines reveals high angle boundaries, while the fine lines correspond to cell-boundaries and sub-boundaries. The area with dense fine lines corresponds to the deformed structure and stored strains, which were developed during cold rolling. Whereas the area with no or little amount of fine lines, which correspond to the low strained grains that were recovered and recrystallized during partial annealing. Figures 6(c) and (d) show the inverse pole figures presenting the orientation of the low strained grains in the partially annealed foils of 3NAl and 4NAl. The red points indicate cube-orientation, while the blue points indicate the grains with other orientations which were recovered and recrystallized during partial annealing. The plots show that most of the strain-free grains in the 3NAl had the β-fiber orientations which were detected in the cold rolled foils. On the other hand, the 4NAl showed many strain-free grains which had the orientations other than β-fiber components. Considering that the typical cold rolled texture consists of the β-fiber orientation, it was expected that, the dislocation density in the grains in the 3NAl would have been reduced by the recovery. While, the strain-free grains in 4NAl were formed not only by the recovery but also by the discontinuous recrystallization. Consequently, the impurities such as Fe and Si would be effective to reduce the mobility of grain boundaries which is necessary to cause the nucleation such as the bulge out mechanism.[17]

3.3 Effect of impurity on the growth of cube-oriented grains in the additionally rolled foils

The OIM images for cube-oriented grains in the surface region of additionally rolled foils of 3NAl and 4NAl[7] were finally annealed at 573 K for 0, 60 and 180 seconds, as shown in Fig. 7. Figure 8 shows the relation between the final annealing time and the area fraction of cube-oriented grains in additionally rolled foils of 3NAl and 4NAl.[7] The values in Fig. 8 indicate the average size of cube-oriented grains.

Before final annealing, the area fraction of cube-oriented grains was 4% in 3NAl and 10% in 4NAl. In both 3NAl and 4NAl, it was recognized that the area fraction of cube-oriented grains in additionally rolled foils were larger than that in partially annealed foils. That could be thought to cause that the temperature of foils would rise during the additional rolling.

The area fraction of cube-oriented grains in 4NAl increased linearly to 38% with final annealing time from 0 to 120 seconds, then increased abruptly at 180 seconds to the area fraction of 95%. While in 3NAl, the area fraction was 28%. Despite the area fraction of cube-oriented grains continued to increase, the average grain size decreased at the annealing time of 180 s. It was caused by the formation of the small cube-oriented grains less than 10 μm in diameter, as shown in the distribution map of 180 s annealed foils in Fig. 7(c). Presumably, cube-oriented grains in the subsurface region grew during the final annealing and eventually emerged on the surface. After the annealing for 600 s, the area fraction of cube-oriented grains in 3NAl became 95% and was as large as that in 4NAl. It was clarified that the area fraction of the cube-oriented grains in both 3NAl and 4NAl increased abruptly after the incubation period, but the incubation period of 3NAl was longer than that of 4NAl. The result suggests that impurities in the aluminum suppress the growth of the cube-oriented grains.

The data described in the previous section suggest that the growth rate of cube-oriented grain depends on the purity. Since the grain growth is brought about by the migration of grain boundaries around the growing grains. Accordingly, it was considered to be of importance to clarify the effect of purity on the mobility and the driving force of the grain growth. It is commonly known that the recovery rate in pure aluminum depends on the purity. Therefore it could be predicted that the residual strain as the driving force of grain growth would depend on the purity. It was also expected that the segregation of impurity to boundaries would reduce the mobility of grain boundaries.[18] Indeed, it was reported that the impurity in pure metals increased the difference of the migration rate between coincidence boundaries and random boundaries.[19] Therefore, it was predicted that the purity

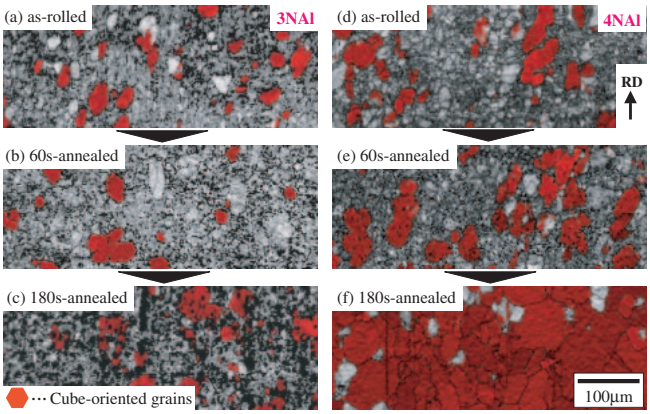

Fig. 7 The OIM images for cube-oriented grains on the surface of the additionally rolled foils of 3NAl, (a) as-annealed, finally annealed at 573 K for (b) 60 and (c) 180 s and the additionally rolled foils of 4NAl,[7] (d) as-rolled, finally annealed at 573 K for (e) 60 and (f) 180 s.

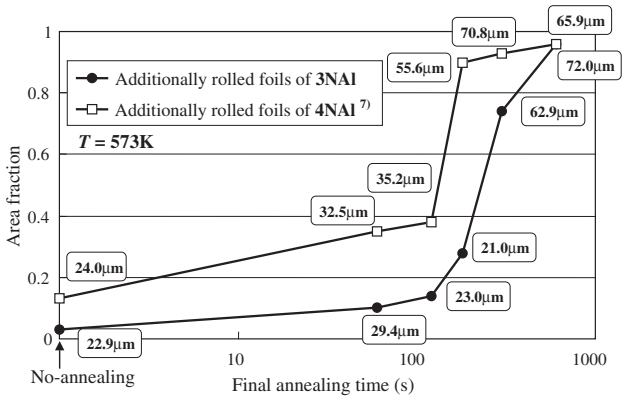

Fig. 8 The relation between final annealing time and area fraction of cube-oriented grains in additionally rolled foils of 3NAl and 4NAl.[7]

Table 1 Vickers hardness (± refers to standard deviation) on the surface of each sample. (Finally annealed foils are additionally rolled foils after 573 K-600 s final annealing).

	Hot rolled sheets	Cold rolled foils	Partially annealed foils	Additionally rolled foils	Finally annealed foils
3NAl	29.38 ± 0.74	37.06 ± 0.15	25.24 ± 0.63	30.14 ± 0.56	20.56 ± 0.48
4NAl	27.96 ± 0.78	36.54 ± 0.49	24.10 ± 0.88	30.06 ± 1.72	20.58 ± 0.37

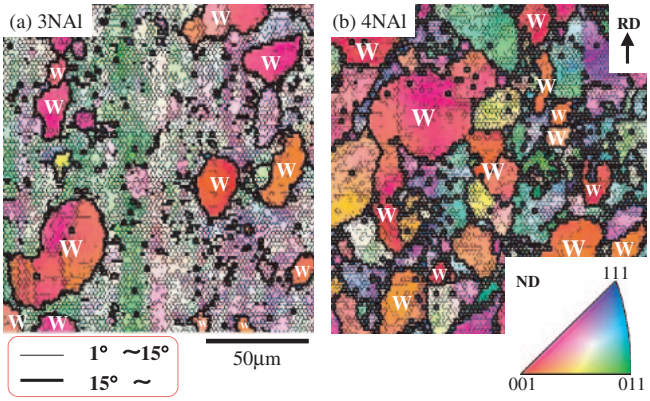

Fig. 9 The distribution of local orientation differences in additionally rolled foils of (a) 3NAl and (b) 4NAl, "W" shows cube grains.

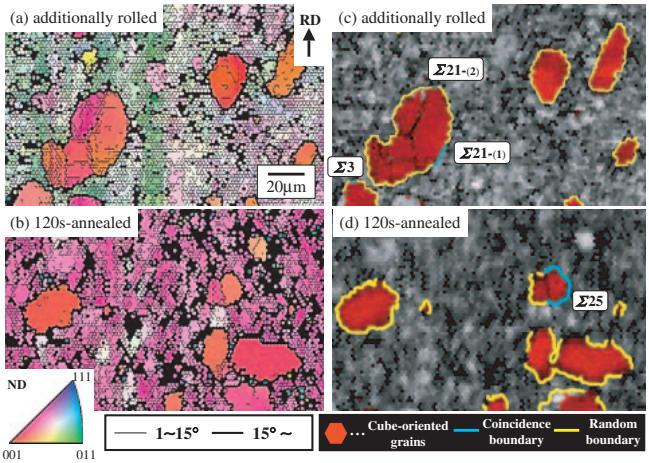

Fig. 10 The OIM images for (a), (b) crystal orientations and (c), (d) cube-oriented grains and grain boundary characters in the surface of additionally rolled and finally annealed foils of 3NAl.

would alter the character of grain boundaries which contribute to the grain growth. Accordingly, from these predictions about the influence of purity on the grain growth, further investigation was carried out to make clear the reason why the purity of aluminum affected the growth of cube-oriented grains.

Table 1 shows the Vickers hardness values of 3NAl and 4NAl at each process. The Vickers hardness of the additionally rolled foils of 3NAl was approximately identical with that of 4NAl. Thus, it was found that the stored strains in foils were about the same in both 3NAl and 4NAl.

Figure 9 shows the OIM images representing the difference of local orientation in the additionally rolled foils of 3NAl and 4NAl. The fine lines indicate the misorientation angle ranging from 1 to 15 degrees, and the bold lines indicate the misorientation angle over 15 degrees. As mentioned in Figs. 6(a) and (b), the fine lines in the same grain can correspond to the amount of stored strains induced by the additional rolling. From the maps, it was observed that

Table 2 Deviation angles from ideal common axes and ideal rotation angles of the coincidence boundaries in Fig. 10.

Coincidence boundaries in Fig. 10	Deviation angle from ideal common axis	Deviation angle from ideal rotation angle
Σ3 (60.0° ⟨111⟩)	5.7°	1.1°
Σ21 - (1) (44.4° ⟨112⟩)	2.6°	1.2°
Σ21 - (2) (44.4° ⟨112⟩)	2.4°	2.0°
Σ25 (51.7° ⟨133⟩)	2.6°	1.8°

all of the cube-oriented grains, which are indicated as "W", were surrounded by high-angle boundaries. And there were less fine lines in the cube-oriented grains than the other grains. Therefore, it was considered that the additional rolling preferentially introduced strains in the grains with different orientation from the cube-orientation. This tendency was confirmed in both 3NAl and 4NAl. It could be thought that cube-oriented grains had the property that the work hardening was difficult to occur, because the eight of all twelve primary slip systems had the same value of Schmid factor, which correspond to cross slip systems.[20] From these results, it could be concluded that the strain would hardly accumulate in cube-oriented grains by the additional rolling and that the difference of purity would not influence the anisotropy of deformation by the additional rolling. Consequently, it was clarified that the quantities and local difference of residual strains in the additionally rolled foils did not depend on the purity.

Figure 10 shows the OIM images representing the difference of local orientation of the additionally rolled foils of 3NAl and the foils finally annealed at 573 K for 120 seconds. In Figs. 10(a) and (b), The fine lines indicate the misorientation angle ranging from 1 to 15 degrees, and the bold lines indicate the misorientation angle over 15 degrees. And in Figs. 10(c) and (d), the blue lines and the yellow lines around cube-oriented grains indicate the coincidence boundaries and random boundaries, respectively. And Table 2 shows the deviation angles from ideal common axes and ideal rotation angles of the coincidence boundaries in Fig. 10. These maps showed that most of the grain boundaries around cube-oriented grains did not have the special orientation relation with adjacent grains in the additionally rolled foils. The same feature remained in the foils annealed at 573 K for 120 seconds. The results showed that the growth of cube-oriented grains in the additionally rolled foils of 3NAl was caused by the migration of random boundaries. Ikeda *et al.* reported the same result in 4NAl.[7] It was clarified that purity did not influence the character of grain boundaries which contribute to the growth of cube-oriented grains.

From these investigations, it could be concluded that cube oriented grains grew by the migration of random boundaries mainly using stored strains energy as the driving force and that purity did not affect the process. Consequently, it was suggested that the segregation of impurity at the random boundaries lowered the mobility of grain boundaries, hence the growth rate of cube-oriented grains was reduced.

4. Conclusions

In the present work, the aluminum foils of different purity (3NAl and 4NAl) after each process for the electrolytic capacitors were analyzed by the SEM/EBSP method. From the results, we discussed the influence of purity on the formation of cube texture. The results are summarized as follows.

(1) In the hot rolled sheets of both 3NAl and 4NAl, there were cube-oriented grains along rolling direction on the surface layer and the center layer. Size and number of the cube-oriented grains in 4NAl were larger than those of 3NAl.

(2) In the cold rolled foils of both 3NAl and 4NAl, β-fiber as the typical rolled texture formed. There were a few cube-oriented grains whose size is about 3 μm. But cube-oriented grains in 4NAl distributed more widely than in 3NAl.

(3) Most of coarsened grains during the partial annealing were characterized by the cube-orientation and β-fiber orientation in 3NAl. On the other hand, there were many coarsened grains of the other orientation in 4NAl. It was expected that dislocation in the grains reduced by the recovery and these grains grew in 3NAl, while the coarsened grains formed by not only the recovery but also the discontinuous recrystallization in 4NAl.

(4) In the additionally rolled foils, cube texture in 4NAl formed faster than in 3NAl during the final annealing. It was clarified that impurity would suppress the growth of cube-oriented grains, while it had no influence on the residual strains and the grain boundary character that controls the preferential growth of cube-oriented grains.

Acknowledgements

The authors would like to thank Mr. K. Tumagari (Graduate School Student, Present address: Sony Semiconductor Kyushu Corporation) for his cooperation in the experiment. This work was conducted as one of the joint researches in the Branch Research Committee on Physical Metallurgy Related to Grain Boundaries, Japan Institute of Light Metals, and the authors wish to thank the committee members for supplying the samples. The part of this work was financially supported by the Grant-in-Aid for Scientific Research from the Ministry of Education, Culture, Sports, Science and Technology and by Light Metal Educational Foundation Inc. They are very much appreciated.

REFERENCES

1) H. P. Kneynsberg, C. A. Verbraak and M. J. T. Bouwhuijs: Mater. Sci. Eng. **72** (1985) 171–176.
2) K. Yamaguchi: J. JILM **35** (1985) 365–371.
3) H. Fukutomi and T. Kamijyo: J. JILM **47** (1997) 123–130.
4) T. Takahashi, T. Murakami and N. C. Danh: J. JILM **28** (1978) 35–40.
5) F. Seki and T. Kamijo: J. JILM **48** (1998) 507–510.
6) T. Kamijo, F. Seki, H. Tamai and K. Ito: J. JILM **49** (1999) 589–594.
7) K. Ikeda, K. Tumagari, F. Yoshida, H. Nakashima and H. Abe: J. JILM **51** (2001) 119–124.
8) O. Engler and M. Y. Huh: Mater. Sci. Eng. A **271** (1999) 371–381.
9) K. Kajihara, K. Tokuda, Y. Sugizaki and Y. Seki: J. JILM **51** (2001) 182–187.
10) M. Kobayashi, Y. Takayama and H. Kato: J. JILM **52** (2002) 547–552.
11) D. G. Brandon: Acta Metall. **14** (1966) 1479–1482.
12) W. Bollmann: *Crystal Defect and Crystal Interfaces*, (Springer, Berlin, 1970).
13) J. Hirsch and K. Lucke: Acta Metall. **36** (1988) 2863–2882.
14) D. Raabe: Acta Metall. **43** (1995) 1023–1028.
15) H. Yamagata: Acta Metall. **43** (1995) 723–729.
16) S. Endo and H. Inagaki: J. JILM **52** (2002) 167–173.
17) J. B. Bailey and P. B. Hirsh: Proc. R. Soc. London, Sect. A **67** (1962) 11–30.
18) D. W. Demianczuk and K. T. Aust: Acta Metall. **23** (1975) 1149–1162.
19) K. T. Aust and J. W. Rutter: Trans. Metall. AIME **215** (1959) 119–126.
20) M. Tagami, K. Kashihara, T. Okada and F. Inoko: J. Japan Inst. Metals **64** (2000) 535–542.